Chapter 1
Laser-Assisted Manufacturing: Fundamentals, Current Scenario, and Future Applications

C. P. Paul, Atul Kumar, P. Bhargava and L. M. Kukreja

Abstract This chapter presents the basic principles, applications, and future prospects of various laser-assisted manufacturing techniques used for material removal, joining, and additive manufacturing. The laser hazard and safety aspect is also briefly included.

1.1 Introduction

The principle of the laser was first known in 1917, when physicist Albert Einstein described the theory of stimulated emission. However, the first laser was practically demonstrated by Theodore Maiman of Hughes Research Laboratories on May 16, 1960 in the form of ruby laser [1]. But this technical break through was dubbed as "solution looking for problems" during early years after the invention. Following the invention of the ruby laser, many other materials were found that could be used as the basis of laser action, such as sapphire, neodymium, and organic dyes such as rhodamine 6G. There were also different ways to excite various compounds to the point of lasing, such as certain chemical reactions, or the acceleration of free electrons to very high energy levels. Today, the laser's presence in the world is ubiquitous [2]. The lasers can heat and vaporize any material, drill holes in the hardest materials—diamond, it can create conditions similar to those on the surface of sun in the laboratory, it can cool the atoms to temperatures almost close to absolute zero, it can measure various parameters with exceptional accuracy, and it can detect impurity. Its continual expansion of the boundaries of science, medicine, industry, and entertainment has resulted in many wonderful applications. Smart bombs, supermarket bar code readers, fiber-optic

C. P. Paul (✉) · A. Kumar · P. Bhargava · L. M. Kukreja
Laser Material Processing Division, Raja Ramanna Centre
for Advanced Technology, PO: RRCAT, Indore, MP 452013, India
e-mail: paulcp@rrcat.gov.in

J. P. Davim (ed.), *Nontraditional Machining Processes*,
DOI: 10.1007/978-1-4471-5179-1_1, © Springer-Verlag London 2013

communication, CD/DVD players, laser printers, certain life-saving cancer treatments, or precise navigation techniques for commercial aircraft could only be possible because of lasers. New and popular medical procedures using lasers have enabled to get rid of eyeglasses, removal of unsightly moles, wrinkles, and tattoos, and even streamline bikini lines. In industries, lasers are employed for a variety of material processing, including—cutting, drilling, welding, brazing, surface hardening, cladding, alloying, and rapid manufacturing. Laser-based manufacturing has several advantages over conventional methods. Some of them are listed below:

1. As non-contact process, it is well suited for processing advanced engineering materials such as brittle materials, electric and non-electric conductors, and soft and thin materials.
2. It is a thermal process and materials with favorable thermal properties can be successfully processed regardless of their mechanical properties.
3. It is a flexible process.

Before proceeding further, first, we will briefly discuss how a laser works, what its special properties are, and how these are being exploited for various applications.

1.2 Lasers Basics

LASER is the acronym of light amplification by stimulated emission of radiation and is essentially a source of intense coherent radiation. The laser differs from ordinary source of light in the emission process of radiation. In an ordinary source, atoms or molecules are excited by thermal excitation, for example, electrical discharge which emits photons spontaneously in a random manner. Photons emitted in all directions with no correlation in wavelength, phase, and polarization between them (Fig. 1.1a). In lasers, photons are emitted by stimulated emission—a characteristic process that generates the photons with all properties (namely—wavelength, phase, direction, and polarization) as those of stimulated photons. Thus, the photons get amplified in an orderly manner (Fig. 1.1b).

Now consider a medium with a large number of atoms (molecules), some of which are in the excited state and rest unexcited. Since the photons get absorbed by

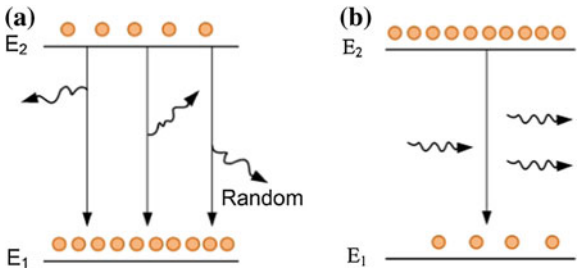

Fig. 1.1 **a** Spontaneous emission. **b** Stimulated emission

the unexcited atoms, the number of excited atoms should be more than that of unexcited atoms for net amplification. This situation is called population inversion. The name is derived from normal trend of the population in the thermal equilibrium, where unexcited atoms are more abundant. Under normal or thermal equilibrium conditions, the lower energy levels are more highly populated than the higher levels ($N_1 > N_2$), and the distribution is given by Boltzmann's law that relates N_1 and N_2 as

$$\frac{N_2}{N_1} = e^{-\frac{E_2 - E_2}{k_B T}}$$

where k_B is Boltzmann's constant $= 1.38 \times 10^{-23}$ J/K and T is the absolute temperature of the system (K). Population inversion ($N_2 > N_1$) though is the primary condition, but in itself is not sufficient for producing a laser. As there are certain losses of the emitted photons within the material itself in addition to spontaneous emission, one has to think about the geometry that can overcome these losses and there is overall gain.

It derives to the following three prerequisites:

- An active medium with a suitable set of energy levels to support laser action.
- A source of pumping energy in order to establish a population inversion.
- An optical cavity or resonator to introduce optical feedback and so maintain the gain of the system overcoming all losses.

In order to create a laser beam from an active medium, that is, the medium in which population inversion is created, the medium is placed between two mirrors (Fig. 1.2). The photons are reflected back and forth by mirrors and get amplified more and more by the active medium. One of the mirrors is partially transmitting through which the laser beam comes out. Stimulated emission and optical resonator arm the laser with certain unique properties. These properties are briefly discussed in the following sections [3, 4].

1. *Monochromaticity*. The energy of a photon determines its wavelength through the relationship $E = \mathrm{hc}/\lambda$, where c is the speed of light, h is Planck's constant,

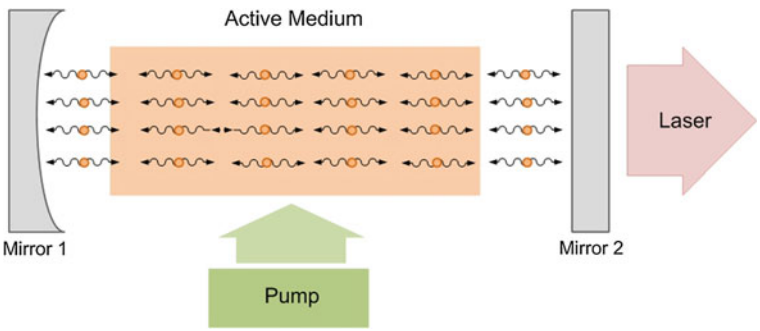

Fig. 1.2 Basic laser system

and λ is the wavelength. In an ideal case, the laser emits all photons with the same energy, thus the same wavelength, and it is said to be monochromatic. However, in all practical cases, the laser light is not truly monochromatic. A truly monochromatic wave requires a wave train of infinite duration. The spectral emission line from which it originates does have a finite width, because of the Doppler effect of the moving atoms or molecules from which it comes. However, compared to the ordinary sources of light, the range of frequency (line width) of the laser is extremely small.

2. *Coherence*. Coherent means that all the individual waves of light are moving precisely together through time and space, that is, they are in phase. Since a common stimulus triggers the emission events, which provide the amplified light, the emitted photons are "in step" and have a definite phase relation to each other. These emitted photons having a definite phase relation to each other generate coherent output, that is, the atoms emit photons in phase with the incoming stimulating photons and emitted waves add to the incoming waves, generating brighter output. Addition is due to the relative phase relationship. Photons of ordinary light also come from atoms, but independent of each other and without any phase relationship with each other and are not coherent. Therefore, laser is called a coherent light source where as an ordinary light is called an incoherent source of light. The concept of coherence can be well understood from the following Fig. 1.3.

There are two types of coherence—spatial and temporal. Correlation between the waves at one place at different times, or along the path of a beam at a single instant, is effectively the same thing and is called "temporal coherence." Correlation between different places (but not along the path) is called "spatial coherence."

3. *Directionality*. One of the important properties of laser is its high directionality. The mirrors placed at opposite ends of a laser cavity enable the beam to travel back and forth in order to gain intensity by the stimulated emission of more photons at the same wavelength, which results in increased amplification due to the longer path length through the medium. The multiple reflections also produce a well-collimated beam, because only photons traveling parallel to the cavity walls will be reflected from both mirrors. If the photon is the slightest bit off axis, it will be lost from the beam. The resonant cavity, thus, makes certain

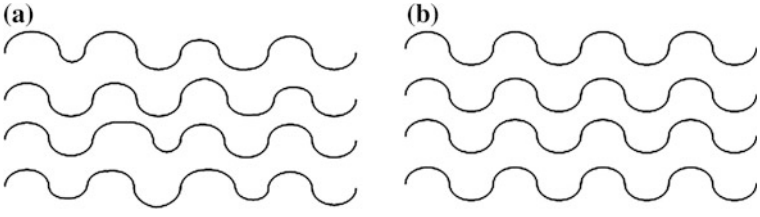

Fig. 1.3 **a** Incoherent. **b** Coherent beam

that only electromagnetic waves traveling along the optic axis can be sustained, consequent building of the gain. The high degree of collimation arises from the fact that the cavity of the laser has very nearly parallel front and back mirrors, which constrain the final laser beam to a path, which is perpendicular to those mirrors. For a laser, the beam emerging from the output mirror can be thought of as the opening or aperture, and the diffraction effects on the beam by the mirror will limit the minimum divergence and spot size of the beam (Fig. 1.4).

From diffraction theory, the divergence angle θ_d is:

$$\theta_d = \frac{\beta\lambda}{D}$$

where λ and D are the wavelength and the diameter of the beam, respectively, and β is a coefficient whose value is around unity and depends on the type of light amplitude distribution and the definition of beam diameter. θ_d is called diffraction-limited divergence.

4. *Brightness*. The brightness of a light source is defined as the power emitted per unit surface area per unit solid angle. A laser beam of power P, with a circular beam cross section of diameter D and a divergence angle θ_d and the result emission solid angle is $\pi\theta_d^2$, then the brightness of laser beam is

$$B = \frac{4P}{(\pi D\theta_d)^2}$$

5. *Focussability*. Focusing of laser beams enables high intensity at the focusing spot. Laser power at the spot and its spot size are some of the crucial parameters during various techniques of laser material processing. Very low divergence of the laser beam allows it to be focused to very small spot $\approx \lambda$
6. *High power*. The accumulated photon density directly depends on the density of excited atoms in active medium and volume of active medium. Higher photon density results in higher laser power.
7. *Short-pulse generation*. Very high powers of lasers are also achieved by different methods of pulse generation/pulse compression techniques. Pulsed laser power in μs, ns, and fs time durations are widely available in MWs, GWs, and

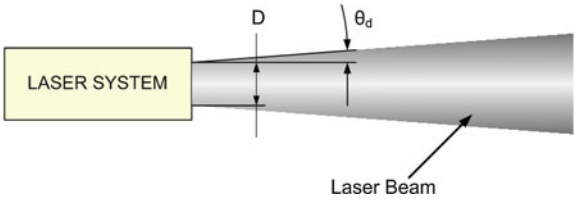

Fig. 1.4 Divergence in laser beam

TWs power ranges while cw laser power is in the range of 10–100 kW. High harmonic generation allows the generation of attosecond pulses with even higher powers of lasers.

1.3 Lasers and Manufacturing Techniques

Though lasers did wonders for advanced applications of science, engineering, and medicine, but they failed in many simple applications. For example, when it was attempted to cut the chocolate candy and slice the bread, the outcomes were burnt charcoal and toast, respectively. These efforts just failed because of incorrect choice of laser and improper selection of processing parameters. Thus, right choice of laser and proper selection of processing parameters are mandatory to realize the applicability and capability of a laser in any application.

Figure 1.5 presents the schematic arrangement of a typical laser processing station. The system shows a laser integrated with a beam delivery system. The beam delivery system may be optical-fiber based or reflecting optics based. The optical-fiber-based beam delivery system is preferred over reflecting optics based due to ease of operations during the material processing. Various CNC laser workstations are used for the beam or job manipulations during laser material processing. Robots are not very common in laser processing due to inferior position accuracy. Among CNC workstations, 3-axis interpolation (*X*, *Y,* and *Z*) is sufficient to reach to any point in the space, but two more axes (*A* and *C*) are required to orient particular direction to reach. Therefore, 3-axis configuration is minimum system requirement and 5-axis is universal requirement without redundancy. Apart from axes-movements, laser workstation needs some more features, like laser on/off, gas on/off, powder feeder on/off, for laser rapid manufacturing (LRM). Depending upon the applications, various processing heads are used. The processing heads for cutting, welding, and cladding are different and specific to the applications. For the consolidated control of the laser material processing, the use of integrated controller is the recent trend.

Though a large variety of lasers employing different kinds of active medium covering a wide range of wavelengths and powers has been developed, only few are being used for material processing. CO_2, Nd:YAG, and fiber lasers are the most popular systems, while excimer and diode lasers are also being employed for various other applications [2, 4]. Table 1.1 presents different type of lasers and their potential application.

In the field of industrial material processing, lasers have given a new direction to cutting of metallic and non-metallic sheets, welding of similar and dissimilar metals and composites, drilling, marking, metal forming, surface hardening, peening, surface alloying, cladding, and rapid manufacturing. Figure 1.6 presents the overview of laser-based manufacturing processes and their process domain in terms of laser power density and interaction time [2, 5]. Consequently, the scenario

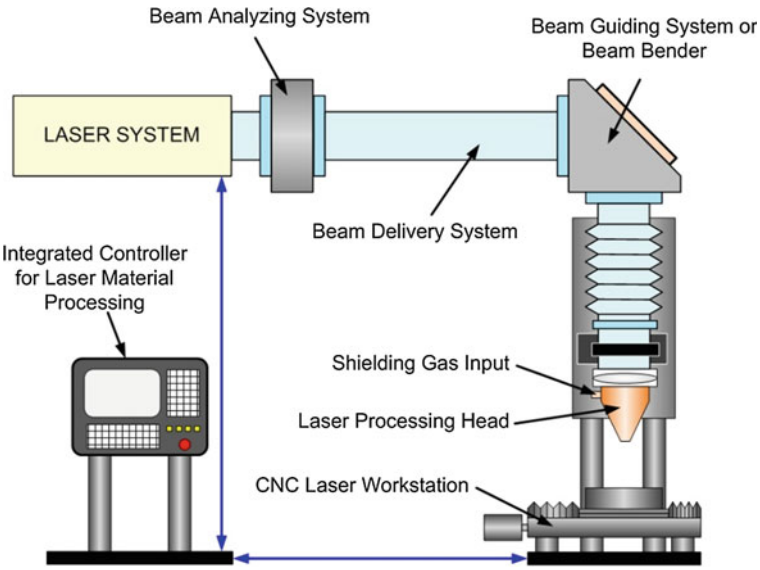

Fig. 1.5 Schematic arrangement of a typical laser processing station

Table 1.1 Different types of lasers and their applications

Laser (wavelength)	Applications
CO_2 laser (10.6 μm)	Light- to heavy-duty industrial cutting, welding, and rapid manufacturing
	Laser surface modification including cladding, alloying, and rapid manufacturing for wear/corrosion resistance and dimensional restoration
	Laser ablation, and laser glazing
Nd:YAG laser (1.06 μm)	Light- to heavy-duty job shops in drilling, welding, cutting, marking, and rapid manufacturing
Fiber laser (1.08 μm)	Laser cleaning in conservation of artifact, paint stripping
Excimer laser KrF (0.248 μm)	Optical stereolithography
XeCl (0.309 μm)	Marking, scribing, and precision micromachining involving drilling, cutting, etching of profile
Copper vapor laser (0.51 μm)	High-speed photography
	Detection of finger prints for forensic applications
	Excitation source for tunable dye laser for isotope separation
	Precision microhole drilling and cutting
Semiconductor laser/ diode laser	Optical computers, CD drivers, laser printers, scanners, and photocopiers
(0.8–1.0 μm)	Optical communication Industrial alignment
	Holography, spectroscopy, bio-detectors, ozone layer detector, pollution detection, bar code scanners, 3D image scanners

in manufacturing has changed, specifically for automobile, chemical, nuclear, and aerospace industries.

1.3.1 Laser Cutting

Laser cutting is one of the largest applications of lasers in metal-working industry and is a well-established universal cutting tool enables cutting of almost all known materials. One of the foremost reasons for wide acceptance of laser cutting was direct replacement of conventional cutting source with laser. When compared with other cutting processes (such as oxy-fuel cutting, plasma cutting, sawing and punching), its advantages are numerous, namely a narrow cut, minimal area subjected to heat, a proper cut profile, smooth and flat edges, minimal deformation of a workpiece, the possibility of applying high cutting speed, intricate profile manufacture and fast adaptation to changes in manufacturing programs [6]. The laser cutting uses different cutting mechanisms to cut different materials. Some of the mechanisms are vaporization, scribing, melt and blow, melt blow and burn, and thermal stress cracking [2].

Vaporization: In vaporization cutting, the focused beam heats the surface of the material to boiling point and generates a keyhole. The keyhole leads to a sudden increase in absorptivity and it results in quickly deepening the hole. As the hole deepens and the material boils, generated vapors erode the molten walls that ejects out the wall material, further enlarging the hole. Organic materials such as wood, Perspex, thermoset plastics, fiber-reinforced plastics are usually cut by this method.

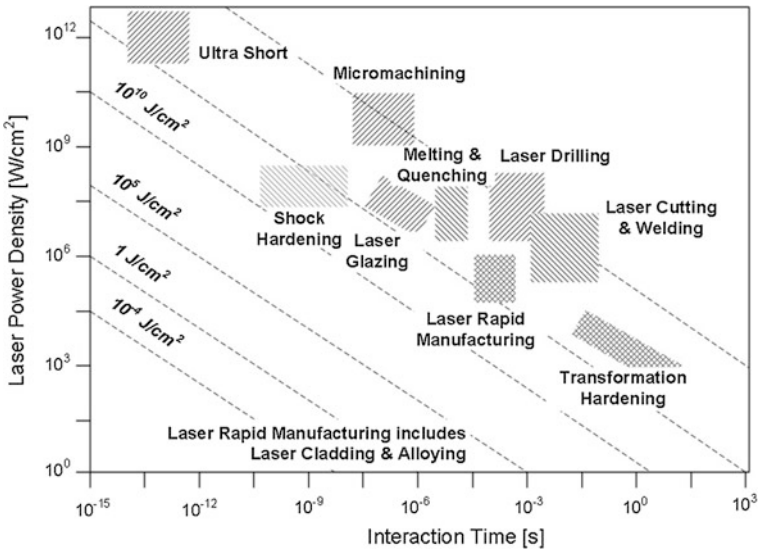

Fig. 1.6 Overview of various laser-based manufacturing processes and their process domain in terms of laser power density and interaction time [2, 5]

Melt and blow: Melt and blow or fusion cutting mode uses high-pressure gas to blow molten material from the cutting area, greatly decreasing the power requirement. First the material is heated to melting point then a gas jet blows the molten material out of the kerf avoiding the need to raise the temperature of the material any further. Materials cut with this process are usually metals. The distinct feature of this cutting mode is that the cut-edge material is same as the base metal and can be put to weld without cleaning the edge. The re-solidified layer has microcrack and ripple along the edge.

Scribing: This mode of cutting involves the drilling of small overlapping hole along the desired cut line by vaporization of the material. The sheet is then crack along the cut line. Generally, hard and brittle materials like ceramics and glass are cut by this mode of cutting.

Melt blow and burn: Melt blow and burn is a reactive cutting. This mechanism is successfully demonstrated in metals especially mild and stainless steel during oxygen-assisted cutting. This mechanism allows the cutting of very thick steel plates with relatively little laser power. The distinct feature of this cutting mode is that there is edge hardening due to existence of oxide and thermal cycle on the cut edge. This mode of cutting is also known as "burning stabilized laser gas cutting."

Thermal stress cracking: Brittle materials are particularly sensitive to thermal fracture, a feature exploited in thermal stress cracking. A beam is focused on the surface causing localized heating and thermal expansion. This results in a crack that can then be guided by moving the beam. The crack can be moved as fast as in order of few m/s. It is generally used in cutting of glasses.

The use of various mechanisms during laser cutting of various materials leads to various advantages over the conventional cutting. The cutting capacity for particular set of processing parameters can be estimated by severance energy (SE). SE is defined as follows:

$$SE = \frac{P}{Vt}$$

where P is laser power (W), V is cutting speed (mm/sec), and t is thickness of the material. The quality of laser cut, that is, width of laser cut or kerf and the quality of cut edges depend upon laser, laser power (average for continuous wave (cw) and peak for pulsed), the motion of laser beam and workpiece. Table 1.2 presents laser cutting kerf width versus material thickness for some of the important engineering materials [7].

With increasing demands of personal customization and to provide variations, the laser cutting with three-dimensional processing is being widely used in interior of cars and high-end buses (most popular application is in roof linings, door, instrument panels, and arm rests), cutting of complex pipe profiles and hydro-formed parts [7, 8]. Most of the parts used in above applications area are primarily made up of polymer-based materials, and hence, the availability of robots resulted in increased popularity of this technology.

Table 1.2 Laser cutting kerf width and material thickness for important engineering materials [7]

Material	Material thickness	Kerf width
Aluminum	2–3 mm	0.2–0.3 mm
Plastics	50–500 μm	2 × beam diameter
Steels	1.5 mm	50 μm
	2.5 mm	150 μm
	3.0 mm	200 μm
	6.0 mm	300 μm

Recent developments in laser systems in terms of power, beam quality, and different novel power modulation schemes have aided in addressing many complex problems of laser cutting in more productive way. Figure 1.7 presents the various profile cutting carried out at the authors' laboratory. The recent studies on the phenomenon of "striation free cutting," which is a feature of fiber laser assisted oxygen cutting of thin-section mild steel, concluded that the creation of very low roughness edges is related to an optimization of the cut front geometry when the cut front is inclined at angles close to the Brewster angle for the laser–material combination [9]. The studies to obtain fine and spatter-free pierced holes at the site of cut initiation along with dross free cut edges of minimum roughness and microstructural changes were also carried out. These studies indicated that suitable close-loop control of duty cycle in proportion to cutting speed in progressive change in pulse duty cycle in proportion to cutting speed will effectively suppress unwanted heating effects at sharp corners of laser cut profiles [10].

1.3.2 Laser Drilling

Since the invention of the laser, there has been a constant development to shorter pulse times. Not long ago 10-ns pulses were the shortest obtainable but now femtosecond lasers are widely applied and even shorter pulses can be obtained in

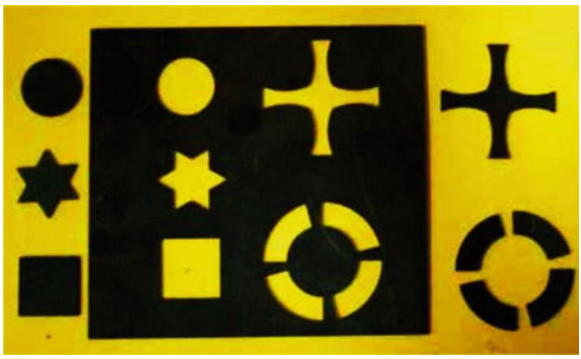

Fig. 1.7 Profile laser cutting carried out at RRCAT

the laboratory. When energy is released in very short time, it results in high peak powers as high as 10^{10} W or orders more. The intensity of the incoming beam is expressed as I_0. The decrease in the laser intensity into the depth of material is given by $I_x = I_0 e^{-\alpha x}$, where α optical absorptivity of the material and x the depth into the material. The optical penetration depth $\delta\,(\delta = 2/\alpha)$ is the depth of material whereby almost all laser energy is absorbed. This optical penetration depth for metals is found to be in the order of 10 nm. It means that the laser energy heats a 10-nm-thick layer of metal in 1 ps. This heat will diffuse from that skin layer (δ) to the bulk. The diffusion depth is expressed by $d = \sqrt{4\,a\,t}$ with a as the thermal diffusivity and t the diffusion time. In case of steel, for 10-fs pulse, we obtain a diffusion depth of 1 nm while during a 1-ps pulse, the heat diffuses over 10 nm. Taking the results together than we see that

- It takes 1 ps to convert laser energy into heat.
- This takes place in a 10-nm-thick skin layer.
- The diffusion depth for 1 ps is also 10 nm.

From these results, we consider a pulse as ultrashort when the (thermal) diffusion depth during the pulse is in the same order or less than the skin layer depth (optical penetration depth). The optical penetration depth depends on the material and the laser wavelength. The diffusion depth depends on the material properties. Table 1.3 presents the ultrashort pulses common for some of the important engineering materials.

When very short pulsed laser beam is focused on any metallic surface, it simply ablates the thin layer of material due to very high power density. The single or repetitive use with appropriate position of focal spot of such pulse results in drilling. In terms of process technology, this technology can be deployed in four ways: single-pulse drilling, percussion drilling, trepanning, and helical drilling. Figure 1.8 presents the schematic diagram of these processes.

In single-pulse drilling, the hole is created in single pulse. Since the drilling is depending on single pulse, the pulse duration and beam profile plays a vital role. The attainable depths in single-pulse drilling range from several micrometers for nanosecond pulse and several millimeters for microsecond pulse. For drilling, higher depth repetitive pulses with appropriate position of focal spot are used and this process is known as percussion drilling. For drilling holes greater than the focal spot and of non-circular shape, the laser beam spot is translated in the profile plan and this drilling process is called laser trepanning. Helical drilling is special

Table 1.3 Ultrashort pulse for some of the important engineering materials [7]

Material	Ultrashort pulse
Metal	1 ps
Ceramic	10 ps
Plastic	1 ns

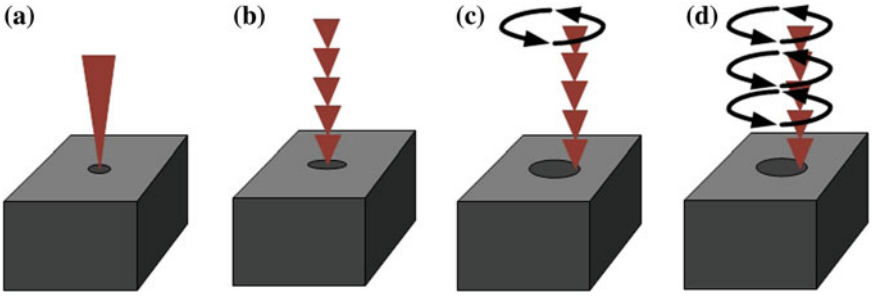

Fig. 1.8 Schematic diagram presenting different drilling processes **a** single drilling **b** percussion **c** trepanning, and **d** helical drilling

case of laser trepanning when the focal spot of laser beam is positioned appropriately along the drilling depth.

Drilling holes on aerospace and avionic components to improve the heat transfer, toil filers of automobiles, are some of the important industrial applications of laser drilling. As compared to electro-eroded and mechanically drilled holes, the laser-drilled holes still have limitations especially in terms of concentricity and burring. Laser drilling is also used in drilling holes in diamond, one of the hardest material on earth. There is difficulty in diamond drilling because it is transparent for a wide range of wavelength. At high power densities, however, the diamond is transformed into graphite, which absorbs the laser power and is removed by ablation subsequently. Diamond machining is currently done by microsecond pulses of Nd:YAG lasers and nanosecond pulses of excimer lasers [11]. Thin layers of graphite or amorphous carbon are found on the surface after laser machining which requires an extra polishing operation to remove the graphite. However, this extra step of polishing can be removed if ultrashort femtosecond lasers are used [12].

In the domain of microdrilling, Excimer lasers are preferred over other lasers, as they offer three significant advantages. First, the short ultraviolet light can be imaged to a smaller spot size than the longer wavelengths. This is because the minimum feature size is limited by diffraction, which depends linearly with the wavelength. The second advantage is that due to the mechanism of "photoablation" there is less thermal influence or melting of the surrounding material. Finally, most materials show a strong absorption in the ultraviolet region. This means that the penetration depth is small and each pulse removes only a thin layer of material, allowing precise control of the drilling depth [8, 13].

One of the exciting applications is fabrication of printed circuit board (PCB), where many bridging holes (vias) are produced to make electrical connections in multi-layer PCBs. The holes are drilled in dielectric polyimide layer until the underlying copper layer is uncovered. The drilling then stops automatically because of the higher threshold (one order of magnitude) of copper. The conducting connection is made by a following chemical deposition of copper on the walls. The process has been developed by Bachmann [14] and is used for drilling

small $\approx$10 μm holes. For bigger holes of 100 μm and above, the cheaper and faster CO_2 lasers are currently used. In the fabrication of nozzle for the ink jet printers, an array of small orifice with precisely defined diameter and taper are required. These holes are located on the top of a channel with resister heater. Small bubbles are formed when the ink is heated, ejecting small (3–80 pl) drops out of the nozzle. Riccardi et al. [15] describes the fabrication of high-resolution bubble ink jet nozzles (similar application is referred in Fig. 1.9). Depending on the design, up to 300 holes have to be drilled simultaneously in a 0.5 × 15 mm area. The total drilling time is about 1 s, using a 300 Hz, KrF laser. Recent developments have facilitated the smaller holes below 25μm diameter for this application.

1.3.3 Laser Welding

When high-power laser beam is focused, it produces very high intensities of the order of 10^4–10^7 W/cm^2 at the focal spot. When such a high-intensity spot is placed on the edges of the materials forming a joint in butt or lap joint configuration, the material melts and solidifies as soon as the beam is passed away. This melting and solidification of the edges under proper shielding result in welding of the material. Among various welding processes, high-energy beam welding employing laser has the key benefits in terms of localized heating, faster rate of cooling, smaller heat-affected zone (HAZ), easier access weld seam through fiber delivery, access to weld intricate geometrical shapes and sizes, reduced workpiece distortion and undulation and possibility of performing welding in ambient and controlled environment [16–21]. The following are main characteristics of the laser-welded joints:

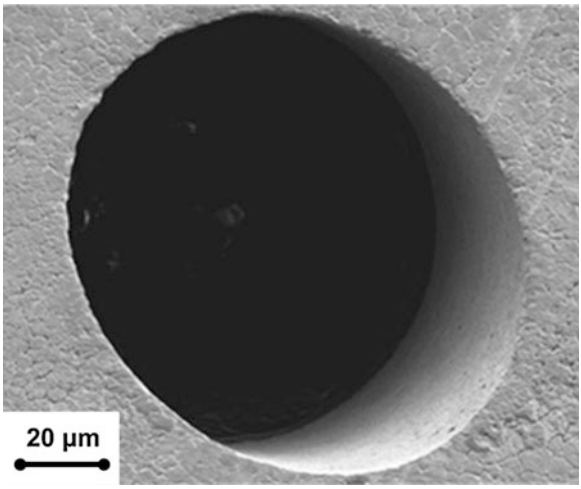

Fig. 1.9 An injection nozzle hole with a high-power picosecond laser produces very sharp edges with no burr or melt and low surface roughness inside the hole, resulting in an optimum spray cloud of the fuel

- Deep and narrow weld.
- Very low thermal distortion and residual welding stresses.
- Narrow HAZ and minimum metallurgical damage.
- High speed and high production rate.
- High precision control in space and energy.
- Autogenous welding, that is, no-filler is required.
- Possibility of dissimilar material joints.
- Welding of relatively remote- and limited-access locations.
- Easy to automate.

Because of these distinguished advantages, it is widely employed for welding coarse to fine precision of thick to thin metals, ceramics, and polymers. The applicability and preference of laser welding depends on laser properties and parameters, material properties and methodology, but the selection of welding joint is broadly governed by the functionality of components. There are few limitations of the laser welding:

- Close fitting of joints and accurate beam/joint alignment is required.
- Precision control of laser and process parameters are required.
- Fixed and running cost of the laser welding machines is high.

To form a laser weld, the laser beam is finely focused on the center line of the joint. Initially most of the incident laser power (even more than 90 %) is reflected, since at the room temperature, metals are good reflector of the infrared radiation. As the metal surface is heated, the surface reflectivity decreases until at the boiling, where it is negligible. The laser energy is absorbed in the skin depth and depending upon the power intensities, two different modes of the laser welding takes place. One is conduction welding and another is keyhole welding. When the material thickness is small and the intensity of the incident laser is relatively low, the material melts and temperature does not exceed the boiling temperature of the material. The aspect ratio (ratio of weld bead height to width) of the weld bead is between 1 and 1.5 for this mode of laser welding. When the power intensities are sufficiently high to cause the vaporization of the material, a hole is created at the center of the molten pool by rapidly escaping metal vapors. In this case, the laser beam further melts and vaporizes the material at the bottom of the created hole. Thus, a narrow hole is formed along the depth of the material. There is dynamic equilibrium among the molten metal, escaping vapor, heat input due to laser, and associated heat transfer phenomena. At the trails edge of the keyhole, the molten material collapses and solidifies forming a deep penetration welding. This mode of welding leads to high aspect ratio in the range of 6–10 (Fig. 1.10).

There has been an extensive experimental and modeling efforts giving insight into laser welding process and associated control for quality and repeatability. In laser welding, when metal melts, its volume increases due to thermal expansion and it forms a convex-shaped weld bead after solidification. The improper selection of

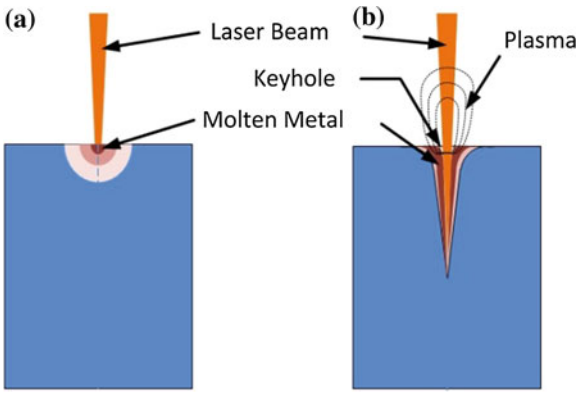

Fig. 1.10 Schematics of **a** heat conduction and **b** deep penetration welding

process parameters results in humping. In humping, there is periodic formation of convex and concave weld bead formation (Refer Fig. 1.11 for details) [22].

In many applications, this protruding convex-shaped weld bead is not acceptable. This can be reduced by appropriate edge preparation. In one of the recent efforts, the size and shape of the edge preparation were estimated experimentally in the authors' laboratory. 6-mm-thick sample of austenitic stainless steel-type 304 (size 15 × 100 mm) having chamfered edges with an included angle of 60° at various chamfered depth ($d = 0.5$, 0.8 and 1.0 mm) was used for the investigation. The detail of chamfered edges is presented in Fig. 1.12. During laser welding, the molten material has tendency to escape away from the molten pool due to its dynamics. Figure 1.13 presents the typical flow molten metal in the molten pool during laser welding. The selected chamfered edges provided a wider wetting surface and easy expansion of the molten material. The depth of the chamfered is selected to provide the compensation to convexity. Table 1.4 presents the results of the laser welding experiments. Fig. 1.14a and b presents the top view of weld sample without chamfered edges and with 0.8-mm-deep chamfered edges, respectively.

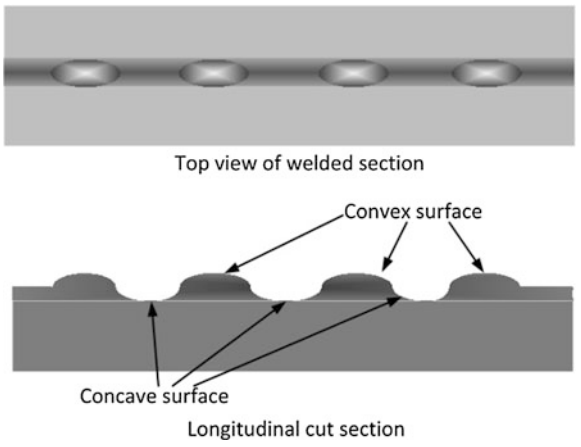

Fig. 1.11 Schematic diagram of humping

During the laser welding, there is angular distortion of the plates due to heating and cooling of the material near the weld zone. There have been several theoretical and experimental studies to predict the distortion [23, 24]. These studies are the extension of the similar studies carried out for the conventional welding processes. For butt-joint configuration, the distortion can be minimized by suitably selecting the proper joint geometry. The angular distortions of 6-mm austenitic stainless steel 304 plates were also studied, and an alternative methodology for minimizing distortion in butt-joint configuration was developed recently in authors' laboratory. Laser welding in butt-joint configuration for the sample with and without chamfered edges was carried out. It was found that the angular distortion for the samples with edges was significantly lesser than that of without chamfered edge. The angular deformation of laser-welded joints having different depth of chamfered edges as a function of laser energy per unit length is shown in Fig. 1.15. Minimum distortion was obtained with 0.8 mm groove depth with laser power per scan speed of 145 kJ/m. For further reduction in the angular distortion, the laser welding was tried from both top and bottom sides. Negligible angular distortion was obtained for both sides welding. The effect of groove on deformation is presented in Fig. 1.16a and b. It is just because the thermal stresses generated during the laser welding cancels each other when welded from the both sides.

Recently, a new approach of laser welding was reported by Fraunhofer IWS Dresden to weld dissimilar materials such as aluminum/copper, aluminum/magnesium, or stainless steel/copper clearly showing better quality [25]. They deployed a highly dynamic 2D scanner with high scanning frequency (up to 2.5 kHz) to generate extremely small weld seam with high aspect ratio. This leads to very short melt pool lifetime, thereby suppressing the formation of brittle intermetallic phases. In these experiments, the melting behavior of metallic mixed joint, seam geometry, chemical composition, melt pool turbulence, and solidification was controlled by high frequency, time, position, and power-controlled laser beam oscillation. Using this strategy, phase seam values less than 10 μm was obtained for the aluminum/copper dissimilar joint. The tensile strength of this dissimilar joint was found to be same value as that of aluminum/aluminum joint [25].

1.3.4 Laser Brazing

Dissimilar metals are preferred due to better material utilization with improved functionality in many engineering applications. It has encouraged the research thrust on various brazing processes including laser brazing. Among the various

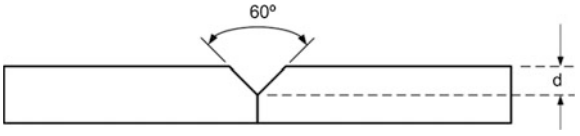

Fig. 1.12 Details of chamfered edges preparation (d = depth of groove)

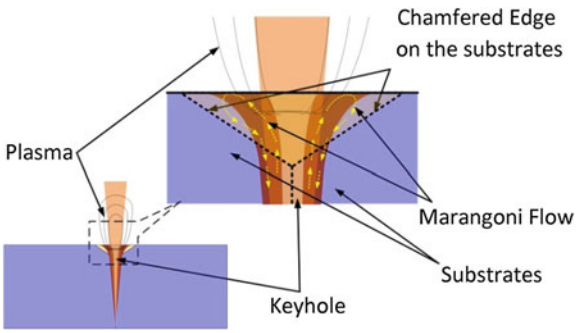

Fig. 1.13 Typical Marangoni flow of molten metal due to chamfered edge during laser welding

Table 1.4 Observed weld bead profile at various processing parameters during laser welding at authors' laboratory

S. No	Laser power (kW)	Scan speed (m/min)	Groove depth (mm)	Observed profile of weld bead
1	2	0.7	Without groove	Convex
2	2	0.8	Without groove	Convex
3	2	0.9	Without groove	Convex
4	2	1.0	Without groove	Convex
5	2	1.1	Without groove	Convex
6	2	0.7	1 mm	Small convex
7	2	0.8	1 mm	Flat
8	2	0.9	1 mm	Concave
9	2	1.0	1 mm	Concave
10	2	1.1	1 mm	Concave
11	2	0.5	0.8 mm	Concave
12	2	0.6	0.8 mm	Concave
13	2	0.7	0.8 mm	Flat
14	2	0.8	0.8 mm	Small convex
15	2	0.9	0.8 mm	Convex
16	2	1.0	0.8 mm	Convex
17	2	1.1	0.8 mm	Convex
18	2	0.7	0.5 mm	Convex
19	2	0.8	0.5 mm	Convex
20	2	0.9	0.5 mm	Convex
21	2	1.0	0.5 mm	Small concave
22	2	1.1	0.5 mm	Concave

combinations of materials, Cu-SS combination is important as Cu has higher thermal conductivity while SS has higher strength. This joint finds application in many advanced engineering applications, like particle accelerators and power plants where efficient removal of heat is mandatory along with material strength. Joining of AISI-type 304L stainless steel with copper using conventional processing portrays multi-fold problems due to the difference in thermophysical properties, while it is challenging for laser processing due to high reflectivity of Cu

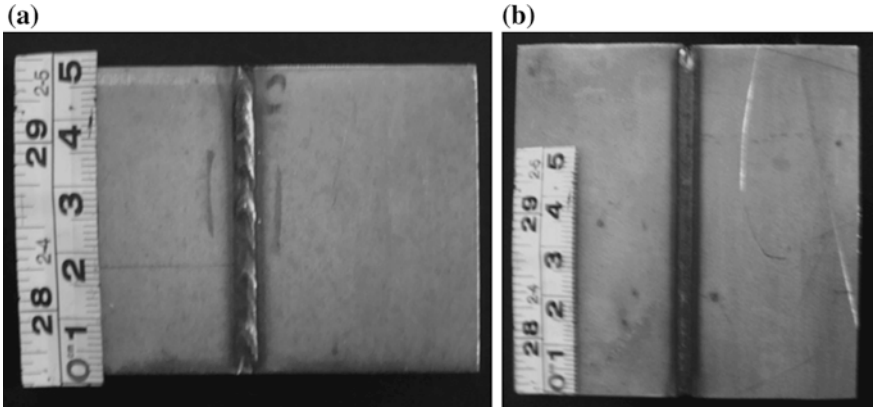

Fig. 1.14 **a** Weld bead without groove and undulation. **b** Weld bead With groove and controlled undulation

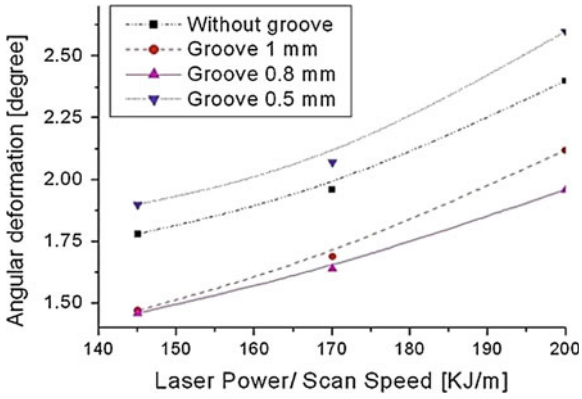

Fig. 1.15 Angular deformations at different laser energy level per unit length

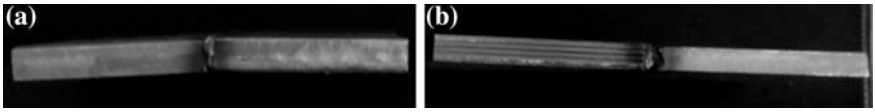

Fig. 1.16 **a** Side view of welding sample without chamfered edge exhibiting the angular distortion. **b** Side view of welding sample with chamfered edge exhibiting reduced angular distortion

[26, 27]. Various brazing techniques are used to join two dissimilar materials [28–30]. In these processes, the closely fitted materials/parts with filler metal are heated above 450 °C, facilitating molten filler metal to flow into fine gaps by capillary action to form material joint. Conventionally, the brazing is performed in a

controlled atmosphere furnace or in vacuum chamber [31] for the joining of Cu with SS. The furnace brazing is very slow process with the unnecessary heating of whole job at high temperature. This heating may produce high thermal stresses in the parts and can change the surface properties of base materials. Laser is widely used as heat source in many material processing applications, including cutting, welding, cladding, surface treatment, and rapid manufacturing [2, 32, 33]. When this is used for the brazing process, it is called as laser brazing [34–36]. By using laser brazing, very thin and miniature parts can be joined with well-controlled HAZ. In the present study, a 2-kW ytterbium fiber laser integrated with 5-axis workstation was used for laser brazing. A number of samples were brazed with using active brazing filler foil (Ag-63 Cu-35.25 Ti-1.75) of thickness 50 microns in butt-joint configuration. The brazed joints were subjected to various non-destructive (visual and dye-penetrant test) and destructive (microscopic examination, energy-dispersive spectroscopy and four-point bending test) characterization techniques.

Two basic process parameters, that is, laser power (P) and scan speed (v), were varied, and their effect on the brazed joint was studied at authors' laboratory. At laser power below 350 W and moderate scan speed (4 mm/min), the proper melting of brazing foil was not occurred. As we increased the laser power keeping the scan speed constant, the melting of filler foil observed and the brazing of Cu-SS was witnessed with relatively good strength. Experiments were also carried out to evaluate the effect of scan speed at constant laser power (450 W) on laser brazing. It was observed that when scan speed was 6 mm/min, the proper melting of filler foil was not occurred. As the scan speed decreased from 6 mm/min, the melting of foil was observed but still the joint was not good by appearance. As scan speed is reduced to 2 mm/min, the melting of foil was occurred and a better brazed joint was observed. The optimum processing parameters for laser brazing of 3-mm SS-Cu joint was found to be 450 W and 2 mm/min.

A number of non-destructive and destructive tests were carried out to characterize the brazed joints. Visual examination is the preliminary examination carried out after laser brazing to detect surface defects, distortion, bead appearance, lack of penetration, spattering etc. The visual examination for the various brazed joints was carried out and the defect-free joints were taken for further examinations. Dye-penetrate test is also carried out for the selected samples and found them with no leaks. This constitutes one of the most important tests, capable of providing insight into modifications taking place in the material as results of laser processing. The feedbacks received from microstructural analysis are often used for optimizing laser processing parameters. The test can provide wide ranging information, for example, microstructural changes, development of deleterious phases, if any (especially during dissimilar metal welding), extent of laser-affected zone, nature and extent of defects developed in the laser-processed joint. Figure 1.17 presents microscopic examination of typical laser-brazed samples at two laser powers at constant scan speed (2 mm/min).

For microstructural examination, brazed samples were polished by various metallurgical techniques and prepared for energy-dispersive X-ray spectroscopy.

Elemental distribution across the brazed joint was studied through point and line scanning. Cu substrate that is used for the brazing experiments had 99.9 % purity. Figure 1.18 presents the elemental distribution across the laser-brazed joint of SS-Cu. It is evidently clear that Fe signal falls as we move from the SS to Cu. There is rise in Cu signal and a peak of Ag in the middle of SS and Cu. The gradient at the interface is sharp, it reconfirm that there was no dilution of the SS and Cu substrate during the brazing process. The line scan of Ag is displaced toward the Cu, as the wettability of Ag is more on Cu as compared to SS.

To evaluate the joint strength, four-point bending test of the laser-brazed joints were conducted and flexural joint strength was evaluated. Prior to testing of brazed joints, four-point bending test specimen was machined from as-received material for evaluating the flexure strength of the material in as-received condition. Table 1.5 summarizes the results of four-point bending test of material in as-received condition. As the laser energy per unit length is increased, the flexural strength of brazed joint increases. It is because the availability of more energy per unit length will result in proper melting and wetting of the brazed material across the joint. As the thermal conductivity of Copper is more and melting point is lower as compared to corresponding values of Stainless steel. The effect of laser focal spot offset in transverse plane is also investigated. The laser beam was offset by 0.5 mm toward SS and Cu and brazing was carried out. When we offset the laser beam toward the Cu side by 0.5 mm, the flexural strength decreases for the laser-brazed joint at various combination of laser power and scan speed. This is due to the availability of lower laser energy (because of high reflectivity at Cu surface and higher thermal conductivity of Cu material) yielding to insufficient wetting of to-be-brazed surfaces. When the laser beam was offset toward the SS side by 0.5 mm, the flexural strength of brazed joint was decreased as compared to that of with zero offset but the flexural strength was increased as compared to that of with laser beam offset toward the Cu side. This is due to the less reflection of laser beam and less thermal conductivity of SS as compared to Cu yielding to relativity higher wetting. Further, the flexural strength is low as compared to zero offset beam

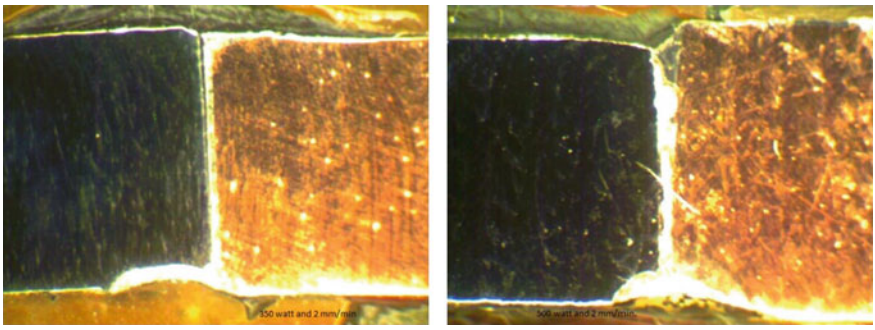

Fig. 1.17 Pictograph of transverse cross section of laser-brazed samples of 3-mm-thick sheets for constant scan speed of 2 mm/min at various laser powers

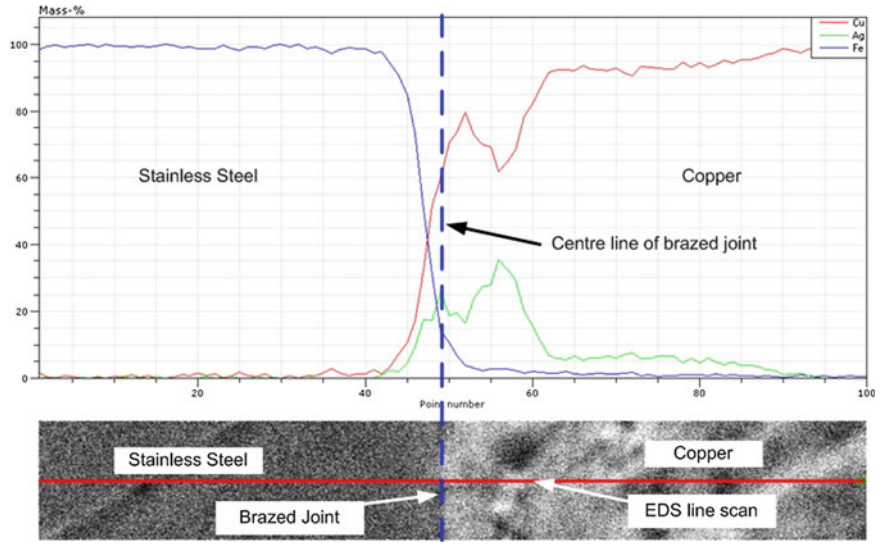

Fig. 1.18 Typical elemental distribution across the laser-brazed joint of SS-Cu

brazing joint because offset of laser beam effects the melting of brazing foil and the heating of contacted surfaces. Results also indicate that the offset of laser beam is very sensitive as it affects the strength of joint. So the alignment and laser beam positioning should be done very carefully (Figs. 1.19, 1.20).

Laser brazing is an attractive technique of joining the material when heat input and subsequent distortion is one of the major criteria for the fabrication of engineering component. In our present study, the laser brazing of Cu and SS was done and the results were compiled. The visual inspection and dye-penetrate testing were done and found that the joint was good. The optical microscopy for the various joints was done. Further, the flexural testing using four-point bending using UTM was carried out and the flexural stresses for different brazed joints were determined and compared with base materials. The scanning electron microscopy was carried out for the various joints and an analysis of the element distribution was performed for material characterization. Maximum flexural stress observed was 343 MPa at the laser power of 550 W and the scan speed of 3 mm/min. If we further increase the laser power, the samples were observed with more

Table 1.5 Results of four-point bending test of material in as-received condition

Sample	Flexural strength [MPa]	Average flexural strength [MPa]
Copper	579.07	506.82
Copper	434.57	
SS 316L	838.83	748.97
SS 316L	659.11	
Brazing foil		450[a]

[a] As per manufacturer's material test report

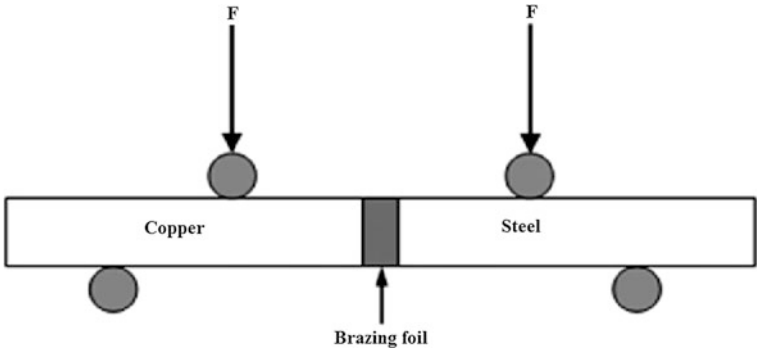

Fig. 1.19 Schematics depicting four-point bending test setup

Fig. 1.20 Effect of laser power and scan speed on flexure strength of brazed joint of 3-mm SS-Cu sheets

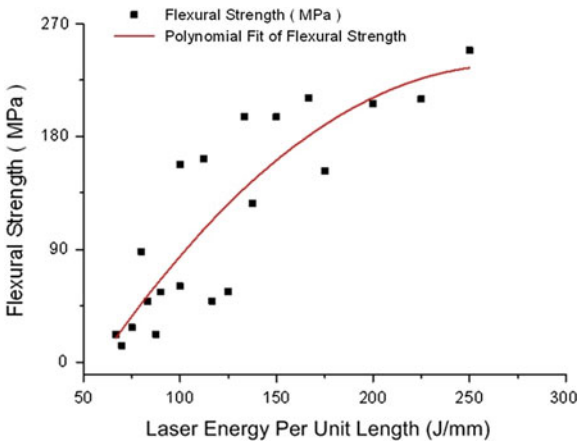

HAZ and some melting of base metal copper was observed at 600-W power with 2- and 3-mm/min scan speeds. At low laser power (less than 350 W), the brazing foil was not melted fully even the scan speed was as low as 2 mm/min. The scanning electron microscopic analysis shows that the diffusion of Ag component of brazing foil is greater in the copper side than SS side.

1.3.5 Laser Rapid Manufacturing

LRM is one of the advanced additive manufacturing processes, that is, capable of fabricating engineering components directly from a solid model. This process utilizes the laser energy as a heat source to melt a thin layer of the substrate together with the blown metal powder to form a layer in a predetermined shape. A number of such layers deposited one over another, and subsequently, it results in fabrication of three-dimensional (3D) components directly from the solid model.

LRM eliminates many production steps such as assembly, man–machine interaction process planning, intermittent quality checks, and consequently related human errors. It also offers many advantages due to its inherent manufacturing features over the conventional subtractive techniques such as reduction in production time and fabrication of functionally graded parts (complex heterogeneous/porous structures). LRM is now put to commercial use for the fabrication of few functional metal parts. Conventional operations show obvious advantages for fabrication of parts in large volume. But when the part is unusual in shape or has fine internal features, the turnaround and cost will increase rapidly, and in some cases, it is impossible to realize. Price is almost secondary to function in some cases. Aerospace, military, space programs, certain marine applications, and biomedical implants come under this category. For these high-value prime applications, LRM is most appropriate. Because of the process flexibility (in terms of raw material selection and feeding), it is possible to make components with compositional grading across length/width to meet the multi-functional requirements. Thus, fabrication of functionally graded materials is one of the important capabilities of rapid manufacturing which finds applications in both the engineering and prosthetic components.

Features that can be attributed to a machine part include the geometry of the part, the material composition, and the microstructure. The material composition is governed by the efficiency of the material delivery method, whereas the microstructure is governed by the specific energy input. As laser-based additive manufacturing techniques can address all these complex issues, manufacturing techniques similar to LRM are being developed with different names at various laboratories around the world. At Sandia National Laboratory, USA, laser engineered net shaping (LENS^{TM}) is being developed with prime focus on creating complex metal parts in single day [37]. National Research Council, Canada, is developing freeform laser consolidation for manufacturing of structural components for advanced robotic mechatronic systems [38]. Automated laser fabrication (ALFa) is being developed to produce low-cost tungsten carbide components at the University of Waterloo, Canada [39]. Selective laser cladding (SLC) at the University of Liverpool, UK, and direct metal deposition at the University of Michigan, USA, are being used for depositing critical surfaces on prime components [40, 41]. Laser powder deposition (LPD) at the University of Manchester, UK, and direct metal deposition/laser additive manufacturing at Fraunhofer Institute, Germany, are being augmented for the fabrication of high-performance materials [42]. The researchers at Tsinghua University, China, are working on diverse area and evaluating the potential of technology for the development of graded Ti alloys for aeronautical, nickel alloys for power plants and various in-situ repair applications [43]. Thus, the ongoing global research is spearheading toward the deployment of the fabrication technology for improving qualities of the products integrated with multi-materials and multi-functional components enhancing a step benefit in economics.

Lasers in LRM: In LRM, high-power laser system is used as heat source to melt thin layer of substrate/previously deposited layer and fed material. CO_2, Nd:YAG,

and diode lasers are most widely used for the application. The availability of high-power fiber lasers made it a new entrant in this application domain [44]. Since the wavelength of Nd:YAG, diode, and fiber lasers are near 1 μm, the absorption is better for laser material processing involving metals as compared to that of CO_2 lasers. However, CO_2 lasers are still being widely used due to less cumbersome safety infrastructure, established systems and procedures. As against the common notion, both pulsed and cw lasers have been successfully used for LRM. The laser energy intensity of 20–60 kW/cm^2 is used for CO_2 lasers, while it is 150–200 kW/cm^2 for pulsed Nd:YAG lasers [45, 46]. The basic prerequisite for laser beam energy intensity distribution is symmetry along the axis of laser beam propagation. It allows uniform material deposition independent of direction of processing. Therefore, multimode laser beam with flat top distribution is most widely used. Gedda et al. compared the laser absorption and the energy redistribution during LRM process using CO_2 laser and Nd:YAG laser [47].

System requirements: LRM system consists of the following three primary subsystems:

1. High-power laser system: One of the following lasers is commonly integrated within the LRM system: CO_2 laser; Nd:YAG laser; diode laser; fiber laser
2. Material feeding system: Among material feeders, there are three main types of feeding techniques. They are wire feeding, preplaced powder bed and dynamic powder blowing.
3. Computerized Numerically Controlled (CNC) workstation: It is either 3- or 5-axes workstation.

The details about the lasers used in LRM systems are already presented in Fig. 1.21. Among the material feeding systems, wire feeders are directly adopted from metal inert gas welding (MIG) process. Wire feeding is preferred for the fabrication of components involve continuous deposition [48, 49], as intermittent start/stops results in discontinuity in deposited material. This method is not adopted as universal method, because of poor wire/laser coupling leading to poor energy efficiency, unavailability of various materials in wire forms and their cost. In preplaced powder bed, a predefined thickness of the powder is laid on the substrate and the powder is melted using laser to form the solidified layer. The method is preferred to fabricate fine features and overhang structures. The method has limitation in achieving cent percent density in the deposits. Dynamic powder blowing is convenient and most widely used approach for material feeding in LRM systems. It allows online variation in feed rate and multi-material feeding. Moreover, laser energy utilization is also more in dynamic powder blowing, as the laser beam passes through the powder cloud to the substrate/previously deposited layer, resulting in preheating of powder particles by multiple reflections. Since the powder is fed into the molten pool for melting and forming layer, some powder particles are ricocheted from the pool. The ratio of the powder deposited to powder fed is termed as powder catchment efficiency. The typical achieved powder catchment efficiency is 35–80 %. In CNC workstations, 3-axis interpolation (*X*, *Y* and *Z*) is sufficient to

reach to any point in the space, but two more axes (*A* and *C*) are required to orient particular direction to reach. Therefore, 3-axis configuration is minimum system requirement and 5-axis is universal requirement without redundancy. Apart from axes-movement, laser workstation needs some more features, like laser on/off, gas on/off, powder feeder on/off, for LRM.

Figure 1.22 presents LRM facility depicting an integrated LRM station with scope for glove box operation to fabricate components in a controlled atmosphere developed at authors' laboratory. Research is underway to incorporate the feedback-based, closed-loop control to precisely manage the temperature, cooling rate, size of the melt pool, and shape of the parts being manufactured. At authors' laboratory, a comprehensive program was undertaken to address various industrial and in-house applications. The fabrication of Colmonoy-6 bushes, solid and porous structures of Inconel-625, and low-cost WC–Co tools are the important applications among them [50–54]. The properties and performance of laser rapid manufactured components/structures are found to be at par with that of conventionally processing component.

Development of high performance surface on SS316L for improved wear resistance: Recently, the studies were extended to the development of high-performance surfaces by depositing tungsten carbide (WC)-reinforced nickel matrix on SS316L. In the study, Inconel-625 alloy (particle size: 45–105 μm) was used to provide nickel matrix for reinforcing WC particles (particle size: 45–75 μm). A number of test trails were made to optimize the processing parameters for LRM of continuous multi-layer overlapped deposition at various powder compositions. It was observed that the deposit got delaminated during the LRM of second layer for 5 % weight Inconel-625 due to insufficient wetting material. This problem was not

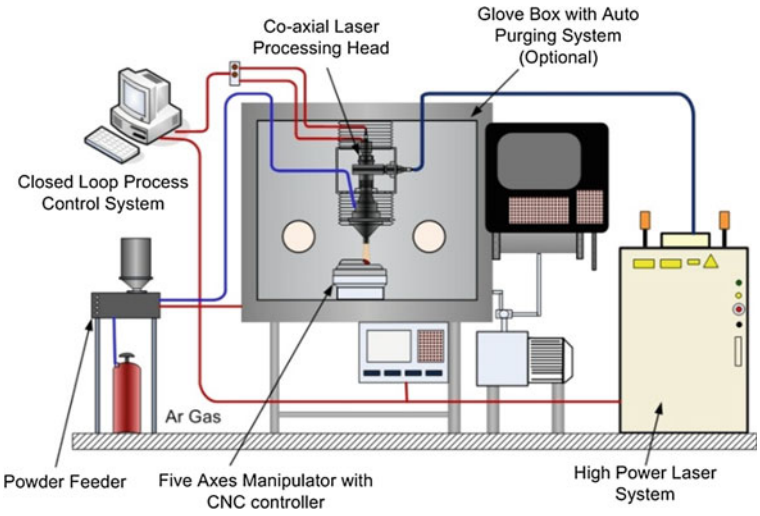

Fig. 1.21 Schematic arrangement of LRM setup

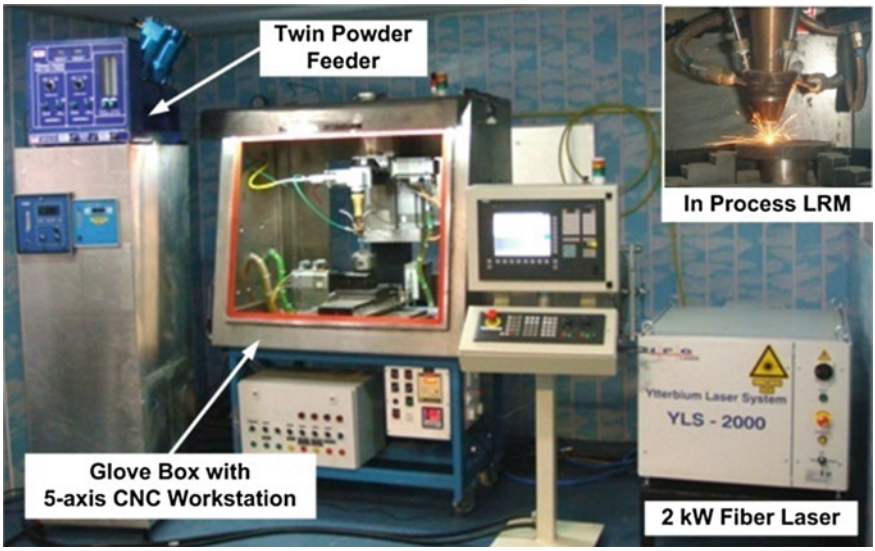

Fig. 1.22 Laser rapid manufacturing facility at author's laboratory

observed for higher compositions. Figure 1.23 presents a typical laser rapid manufactured WC-reinforced nickel matrix on 316L Stainless Steel.

The microscopic examination revealed that the dendritic microstructure of Ni-matrix originated from WC particles due to directional quenching (refer Fig. 1.24). The erosion wear performance of the laser rapid manufactured samples was evaluated using Al_2O_3 air-jet erosion test rig for Inconel-625 in deposit ranging 5–25 % weight, erodent jet velocity ranging 10–50 m/s, jet impinging angle ranging 0–68°, and substrate temperature 50–250 °C. Figure 1.25 presents contours depicting erosion wear rate (EWR) for various composition and impinging angle at erodent velocity 30 m/s and substrate temperature 150 °C. The study demonstrated that WC-reinforced Ni-matrix laser rapid manufactured with

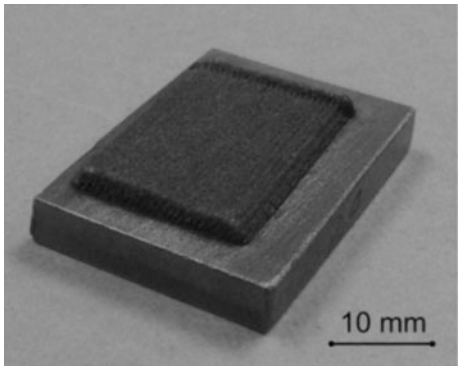

Fig. 1.23 Typical laser rapid manufactured WC-reinforced nickel matrix on 316L SS

18 wt % of Inconel-625 has least EWR for the range of parameters under investigation and it was found to be nine times lower than that of bare SS316L surface.

In another study, high-performance layers of cobalt-free materials were developed and their cavitation and slurry erosion behaviors were studied. The preference to the cobalt-free materials for nuclear applications to avoid induced radioactivity was the main motivation to develop laser cladding of Colmonoy-5 (a nickel base alloy) and Metco-41C (an iron base alloy) on AISI-type 316L stainless steel substrate. The process parameters were optimized for developing continuous and defect-free laser cladding of Colmonoy-5 and Metco-41C on AISI-type 316L stainless steel substrate using dynamic powder blowing methodology (powder particle size used: 45–105 μm). The observed optimum parameters were as follows: laser power: 1.6 kW; scan speed: 0.6 m/min; and powder feed rate: 8 g/min, with 60 % overlap index.

Figure 1.26 presents the typical microstructure at substrate-clad interface for Colmonoy-5 and Metco-41C. X-ray diffraction studies showed the presence of carbides, borides, and silicides of Cr and Ni for Colmonoy-5 whereas Metco-41C cladding exhibited the work hardening microconstituent, that is, austenite. The microstructural studies showed that the clad layers of Colmonoy-5, Metco-41C, and Stellite-6 primarily contain very fine columnar dendritic structure while clad-substrate interface exhibited planar and non-epitaxial mode of solidification due to high cooling rates. Multi-pass cladding showed refined zone at interface due to remelting and solidification. Figure 1.27 presents the microhardness profile for these claddings.

The improvement in cavitation and slurry erosion resistance of laser cladding with respect to AISI-type 316L is summarized in Table 1.6. Metco-41C showed better cavitation and slurry erosion resistance (especially @ 30°) than other cladding used in this work. The improvement in erosion resistance of developed clad layers was primarily attributed to arrest of craters formed by the metal matrix due to high toughness and reasonably good hardness.

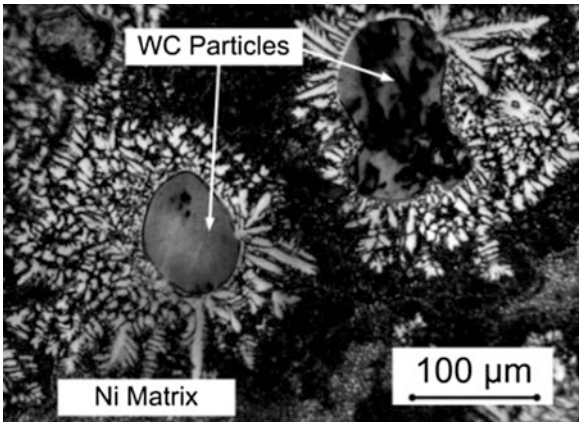

Fig. 1.24 Micrograph depicting the WC particles in nickel matrix with dendrites

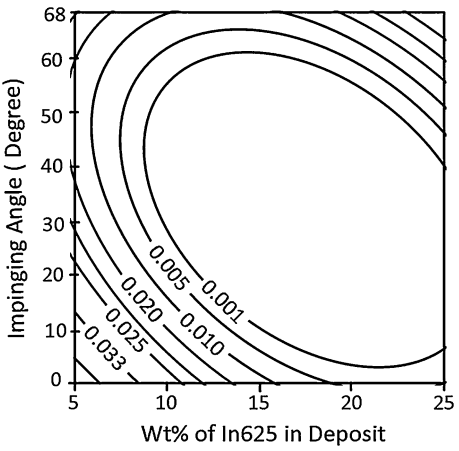

Fig. 1.25 Contours depicting EWR for various composition and impinging angle at erodent velocity 30 m/s and substrate temperature 150 °C

1.4 Laser Hazards and Safety

The lasers have been deployed widely for various manufacturing processes, but there are many laser hazards, and proper arrangements are prerequisite at the shop floor to avoid accidental damage, specifically to human [55]. Excessive levels of laser radiation are hazardous to any exposed area of human body. Because of their susceptibility to damage, the hazards to eye, skin, and the internal organs are different.

The eye hazards deserve special attention because of the particular vulnerability of eye and the extreme importance of sight. The general structure of the human eye is presented Fig. 1.28.

Light passes through the various ocular structures (*C*, *P* and *L*) to fall on the retina (*R*) where it triggers a photochemical process which evokes the neural impulses that leads to the perception of vision. Damage to the eye can occur on any of these structures and depends upon which structure absorbs the greatest

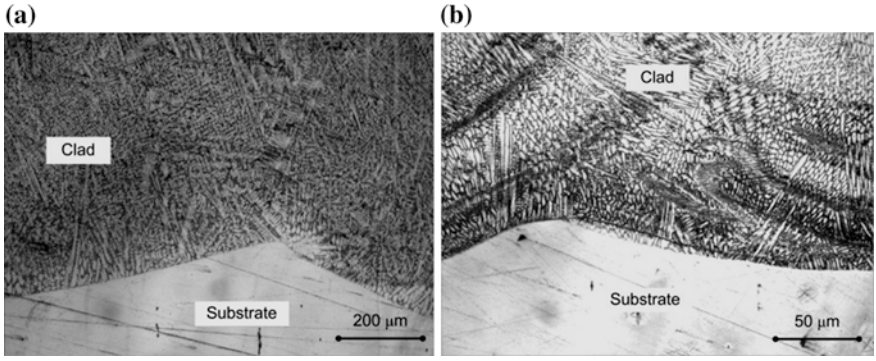

Fig. 1.26 Typical microstructure at clad-substrate interface for **a** Colmonoy-5 and **b** Metco-41C

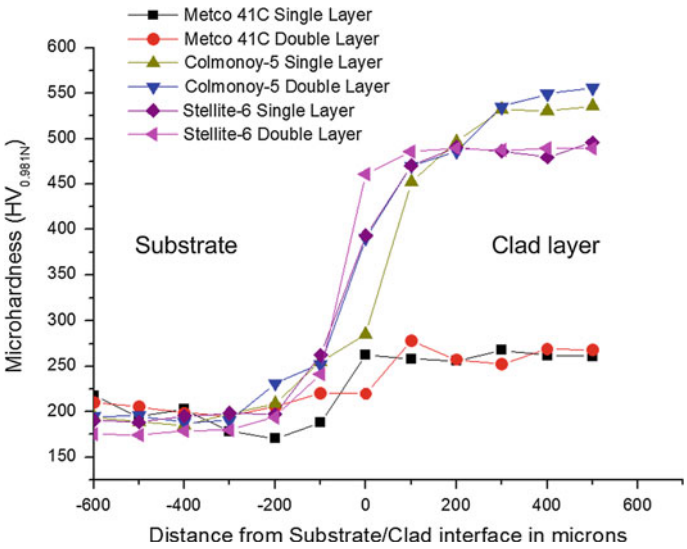

Fig. 1.27 Microhardness across clad-substrate interface for various cladding

Table 1.6 Wear behavior with respect to bare AISI-type 316L stainless steel

Description	Colmonoy-5	Stellite-6	Metco-41C
Cavitation erosion	1.6	4.1	4.6
Slurry erosion @ 30°	1.5	1.75	4.9
Slurry erosion @ 90°	2.2	3.5	2.9

radiant energy per unit volume of the tissue. The ocular media are transparent to radiation in the range 400–1400 nm. All the radiations falling on the cornea in this spectral range will be brought to a focus on the retina resulting very high retinal irradiance and it leads to retinal damage. The laser spot diameter on the retina may be very small ($\sim$1–10 μm), and it results in retinal irradiance up to 10,000 times higher than the corneal irradiance. The typical result of a retinal injury is blind spot within the irradiated area. The cornea is susceptible to damage by ultraviolet radiation (wavelength less than 300 nm) and from infrared radiation. If the injury is restricted to the outer most layers ($\sim$50 μm thick), the injury is likely to be very painful and gets heal within 48 h, it is because the outermost layer of the cornea gets renewed in period of every 48 h. However, the damage to the deeper layer of the cornea results in permanent corneal opacities and thus is very serious hazard.

Hence, the use of appropriate safety goggles in the laser laboratory is primary requisite before any laser experiments [56].

The skin injury thresholds are comparable with that of eye injury thresholds except the retinal injury where the radiation is focused on retina. However, the skin injury is normally very superficial unless incident takes place at very

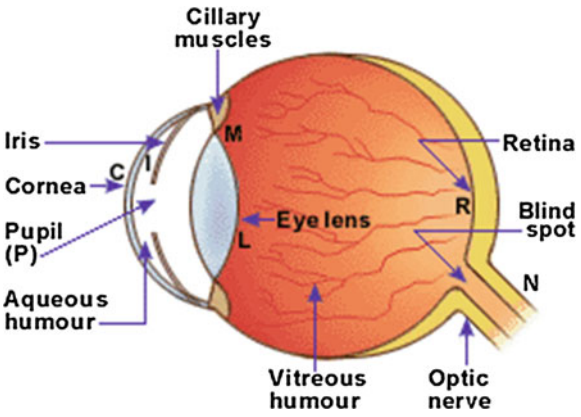

Fig. 1.28 The general structure of human eye

high-power level. It normally involves changes to the outer dead layer of the skin cell. The greater the penetration depth means the greater the volume of tissues available to deposit the absorbed energy. Because of this reason, the damage thresholds for visible and near infrared radiation are higher. Ultraviolet radiation induces photochemical reactions leading to erythema (reddening of skin) and prolonged exposure may initiate longer term degenerative processes, like accelerated skin aging and increased risk of certain type of skin cancer. Hence, appropriate guards and protective screen must be used for laser experiments to avoid direct or indirect exposure to skin.

Hazard to *deep lying organs* are rather unlikely and not generally considered harmful. It is suggested that the thicker hair, scalp, and skull of man would protect the human brain against the focused or unfocused laser beam in the range of 40 J.

Considering the health hazard with the exposure of laser radiation, the following general practices must be used in the laboratory or industry to avoid unwanted incidents [56]:

- Everyone who uses a laser should be aware of the risks. This awareness is not just a matter of time spent with lasers; to the contrary, long-term exposure with invisible risks (such as from infrared laser beams) tends to reduce risk awareness, rather than to sharpen it.
- Optical experiments should be carried out on an optical table with all laser beams traveling in the horizontal plane only, and all beams should be stopped at the edges of the table. Users should never put their eyes at the level of the horizontal plane where the beams are in case of reflected beams that leave the table.
- Watches and other jewelry that might enter the optical plane should not be allowed in the laboratory. All non-optical objects that are close to the optical plane should have a matte finish in order to prevent specular reflections.
- Adequate eye protection should always be required for everyone in the room if there is a significant risk for eye injury.

- High-intensity beams that can cause fire or skin damage (mainly from class 4 and ultraviolet lasers) and that are not frequently modified should be guided through tubes.
- Alignment of beams and optical components should be performed at a reduced beam power whenever possible.

1.5 Conclusion

In manufacturing, the lasers have demonstrated the processing capability with improved quality in all three processing domains: material removal (cutting and drilling), material joining (welding and brazing), and material addition (cladding, alloying, and rapid manufacturing). In material removal, the laser cutting and laser drilling processes could do what was not possible with conventional processing. Deployment of lasers for nuclear decontamination and decommissioning is one of such practical examples. The laser brought the joining process to new height by welding dissimilar materials without sacrificing the relevant mechanical properties. The use of laser brazing also brought the little distortion without compromising the esthetic aspects of the esteemed products, like high-value cars. LRM is an extremely flexible technique with application in multiple areas from repair of large-scale components to manufacturing of component with specific end application. Availability of compact high-power lasers, advanced CAD/CAM systems with faster computing speeds, and advanced diagnostic and control systems has provided a new dimension to manufacturing, and LRM is one of such development. Technical factors, such as advancement in sub-systems, and economic factors, such as falling price of lasers and other sub-systems, will further alleviate the deployment of LRM technology to manufacturing.

With the increased interests from various industries, laser-based manufacturing is likely to lead all fields including aerospace, medical devices, and tooling. In combination with innovative design and planning, the capabilities of laser-based manufacturing have been established to fabricate complex components with delicate details that are very difficult or even impossible to make using conventional manufacturing processes. It does not mean that laser-based manufacturing is a threat to the existence of conventional manufacturing processes, but it is simply going to augment the industries with advanced manufacturing technology to address unresolved complex geometrical and material issues. In combination with other conventional manufacturing processes, laser-based manufacturing is going to provide a unique cost-effective solution to next generation “feature-based design and manufacturing” using the strength of virtual and remote manufacturing. In these ways, these technologies will augment each other to bring the new era of hybrid technologies.

Acknowledgments The authors express their sincere gratitude to Dr. P. D. Gupta, Director Raja Ramanna Centre for Advanced Technology (RRCAT) for his constant support and encouragement. Thanks are due to our collaborators Prof. A. K. Nath of Indian Institute of Technology, Kharagpur, India, and Prof B. K. Gandhi of Indian Institute of Technology, Roorkee, India. During the experimental work presented above, the technical support of Mr. Sohanlal, Mr. A. S. Padiyar, Mr. S. K. Mishra, Mr. C. H. Prem Singh, Mr. M.O. Ittoop, Mr. Abrat Varma, Mr. Anil Adbol, Mr. Ram Nihal Ram, Mr. P Sangale, and Mr. S. K. Perkar of RRCAT and Mr. N. Yadaiah of Indian Institute of Technology, Guwahati, is thankfully acknowledged.

References

1. Bertolotti M (2005) The history of the laser. The Institute of Physics, London
2. Steen WM, Mazumder J (2010) Laser material processing. Springer, London
3. Silfvast WT (2004) Laser fundamentals. Cambridge Press, Cambridge
4. Thyagrajan K, Ghatak A (2010) Lasers: fundamentals and applications. Springer, London
5. Meijer J (2004) Laser beam machining (LBM), state of the art and new opportunities. J Mater Process Technol 149:2–17
6. Dahotre NB, Harimkar SP (2010) Laser fabrication and machining of materials. Springer, London
7. www.obrusn.torun.pl/htm0/prod_images/rofin/Laserbook.pdf. Accessed 9 Dec 2012
8. Ready JF (2001) LIA handbook of laser material processing. Magnolia Publishing, Inc., Magnolia
9. Powell J, Al-Mashikhi SO, Kaplan AFH, Voiseya KT (2011) Fibre laser cutting of thin section mild steel: an explanation of the 'striation free' effect. Opt Lasers Eng 49:1069–1075
10. Kukreja LM, Kaul R, Paul CP, Ganesh P, Rao BT (2012) Emerging laser materials processing techniques for future industrial applications. In: Majumdar JD, Manna I (eds) Laser-assisted fabrication of materials. Springer, London
11. Windholz R, Molian P (1997) Nanosecond pulsed excimer laser machining of CVD diamond and HOPG graphite. J Mater Sci 32:4295–4301
12. Shirk MD, Molian PA (1998) Ultrashort laser ablation of diamond. J Laser Appl 10:64–70
13. Liu L, Chang CY, Wu W, Pearton SJ, Ren F (2013) Circular and rectangular via holes formed in SiC via using ArF based UV excimer laser. Appl Surf Sci 257:2303–2307
14. Bachmann FG (1990) Industrial laser applications. Appl Surf Sci 46:254–263
15. Riccardi G, Cantello M, Mariotti F, Giacosa P (1998) Micromachining with excimer laser. CIRP Ann 47:145–148
16. Quintino L, Costa A, Miranda R, Yapp D, Kumar V, Kong CJ (2007) Welding with high power fiber lasers—a preliminary study. Mater Des 28:1231–1237
17. Kinoshita K, Mizutani M, Kawahito Y, Katayama S (2006) Phenomena of welding with high-power fiber laser. Paper #902 proceedings of ICALEO, pp 535-541
18. Khan MMA, Romoli L, Fiaschi M, Sarri F, Dini G (2010) Experimental investigation on laser beam welding of martensitic stainless steels in a constrained overlap joint configuration. J Mater Process Technol 210:1340–1353
19. Katayama S, Kawahito Y, Mizutani M (2010) Elucidation of laser welding phenomena and factors affecting weld penetration and welding defects. Physics procedia 5:9–17
20. Zhang X, Ashida E, Katayama S, Mizutani M (2009) Deep penetration welding of thick section steels with 10 kW fiber laser. Transactions of JWRI 27:63–73
21. Manonmani K, Murugan KN, Buvanasekaran G (2007) Effects of process parameters on the bead geometry of laser beam butt welded stainless steel sheets. Int J Adv Manuf Technol 32:1125–1133
22. Berger P, Hügel H, Hess A, Weber R, Graf T (2011) Understanding of humping based on conservation of volume flow. Physics Procedia 12:232–240

23. Wang R, Rasheed S, Serizawa H, Murarkawa H, Zhang J (2008) Numerical and experimental investigations on welding deformation. Trans JWRI 37:79–90
24. Deng D, Liang W, Murakawa H (2007) Determination of welding deformation in fillet-welded joint by means of numerical simulation and comparison with experimental measurement. J Mater Process Technol 183:219–225
25. Kraetzsch M (2012) Laser beam welding with high frequency. LIA Today 18
26. Torkamany MJ, Tahamtan S, Sabbaghzadeh J (2010) Dissimilar welding of carbon steel to 5754 aluminum alloy by Nd:YAG pulsed laser. Mater Des 31:458–465
27. Anawa EM, Olabi AG (2008) Optimization of tensile strength of ferritic/austenitic laser welded components. Opt Laser Technol 46:571–577
28. Yoshihisa S, Takuya T, Kazuhiro N (2010) Dissimilar laser brazing of boron nitride and tungsten carbide. Mater Des 31:2071–2077
29. Mai TA, Spowage AC (2004) Characterization of dissimilar joints in laser welding of steel–kovar, copper–steel and copper–aluminium. Mater Sci Eng, A 374:224–233
30. Dharmendra C, Rao KP, Wilden J, Reich S (2011) Study on laser welding–brazing of zinc coated steel to aluminum alloy with a Zinc based filler. Mater Sci Eng, A 528:1497–1503
31. Lippmann W, Knorr J, Wolf R, Rasper R, Exner H, Reinecke A-M, Nieher M, Schreiber R (2004) Laser joining of silicon carbide—a new technology for ultra-high temperature resistant joints. Nucl Eng Des 231:151–161
32. Paul CP, Bhargava P, Kumar A, Kukreja LM (2012) Laser rapid manufacturing: technology, applications, modeling and future prospects. In: Davim JP (ed) Lasers in manufacturing. Wiley-ISTE, London
33. Masato K (2009) Fiber lasers: research, technology and applications. Nova Science, New York
34. Huang S, Tsai H, Lin S (2004) Effects of brazing route and brazing alloy on the interfacial structure between diamond and bonding matrix. Mater Chem Phys 84:251–258
35. Peyre P, Sierra G, Deschaux-Beaume F, Stuart D, Fras G (2007) Generation of aluminium–steel joints with laser-induced reactive wetting. Mater Sci Eng, A 444:327–338
36. Li L, Feng X, Chen Y (2008) Influence of laser energy input mode on joint interface characteristics in laser brazing with Cu-base filler metal. Trans Nonferrous Met Soc China 18:1065–1070
37. http://www.sandia.gov/mst/pdf/LENS.pdf. Accessed on 10 Dec 2010
38. Xue L, Islam MU, Theriault A (2001) Laser consolidation process for the manufacturing of structural components for advanced robotic mechatronic system—a state of art review. In: Proceedings of 6th international symposium on artificial intelligence and robotics and automation in space (i-SAIRAS 2001), Canadian Space Agency, St-Hubert, Quebec, Canada, June 18–22
39. Paul CP, Khajepour A (2008) Automated laser fabrication of cemented carbide components. Opt Laser Technol 40:735–741
40. Davis SJ, Watkins KG, Dearden G, Fearon E, Zeng J (2006) Optimum deposition parameters for the direct laser fabrication (DLF) of quasi-hollow structures. In: Proceedings of photon conference Manchester, Institute of Physics
41. He X, Yu G, Mazumder J (2010) Temperature and composition profile during double-track laser cladding of H13 tool steel. J Phys D Appl Phys 43:015502
42. Moat RJ, Pinkerton A, Li L, Withers PJ, Preuss M (2009) Crystallographic texture and microstructure of pulsed diode laser-deposited Waspaloy. Acta Mater 5:1220–1229
43. Zhong M, Liu W (2010) Laser surface cladding: the state of the art and challenges. Proc Inst Mech Eng Part C: J Mech Eng Sci 224:1041–1060
44. Valsecchi B, Previtali B, Vedani M, Vimercati G (2010) Fiber laser cladding with high content of Wc-Co based powder. Int J Mater Form 3(Suppl):11127–11130
45. Kreutz E, Backes G, Gasser A, Wissenbach K (1995) Rapid prototyping with CO2 laser radiation. Appl Surf Sci 86:310–316
46. Sun S, Durandet Y, Brandt M (2005) Parametric investigation of pulsed Nd:YAG laser cladding of Stellite 6 on stainless steel. Surf Coat Technol 194:225–231

47. Gedda H, Powell J, Wahistrom G, Li WB, Engstrom H, Magnusson C (2002) Energy redistribution during CO2 laser cladding. J Laser Appl 14:78–82
48. Draugelates U, et al (1994) Corrosion and wear protection by CO2 laser beam cladding combined with the hot wire technology. In: Proceedings of ECLAT '94, pp 344–354
49. Hensel F, Binroth C, Sepold GA (1992) Comparison of powder and wire-fed laser beam cladding. In: Proceedings of ECLAT '92, pp 39–44
50. Paul CP, Jain A, Ganesh P, Negi J, Nath AK (2006) Laser rapid manufacturing of Colmonoy components. Opt Lasers Eng 44:1096–1109
51. Paul CP, Ganesh P, Mishra SK, Bhargava P, Negi J, Nath AK (2007) Investigating laser rapid manufacturing for Inconel-625 components. Opt Laser Technol 39:800–805
52. Paul CP, Alemohammad H, Toyserkani E, Khajepour A, Corbin S (2007) Cladding of WC-12Co on low carbon steel using a pulsed Nd:YAG laser. Mater Sci Eng, A 464:170–176
53. Paul CP, Mishra SK, Premsingh CH, Bhargava P, Tiwari P, Kukreja LM (2012) Studies on laser rapid manufacturing of cross-thin-walled porous structures of Inconel 625. Int J Adv Manuf Technol 61:757–770
54. Ganesh P, Moitra A, Tiwari P, Sathyanarayanan S, Kumar H, Rai SK, Kaul R, Paul CP, Prasad RC, Kukreja LM (2010) Fracture behavior of laser-clad joint of Stellite 21 on AISI 316L stainless steel. Mater Sci Eng, A 527:3748–3756
55. http://www.utexas.edu/safety/ehs/lasers/Laser%20Safety%20Handbook-tnt.pdf. Accessed on 9 Dec 2012
56. Barat K (2009) Laser safety: tools and training. CRC Press, Boca Raton